Article

Glycine Enolates: The Effect of Formation of Iminium Ions to Simple Ketones on α-Amino Carbon Acidity and a Comparison with Pyridoxal Iminium Ions

Juan Crugeiras, Ana Rios, Enrique Riveiros, Tina L. Amyes, and John P. Richard

J. Am. Chem. Soc., **2008**, 130 (6), 2041-2050 • DOI: 10.1021/ja078006c

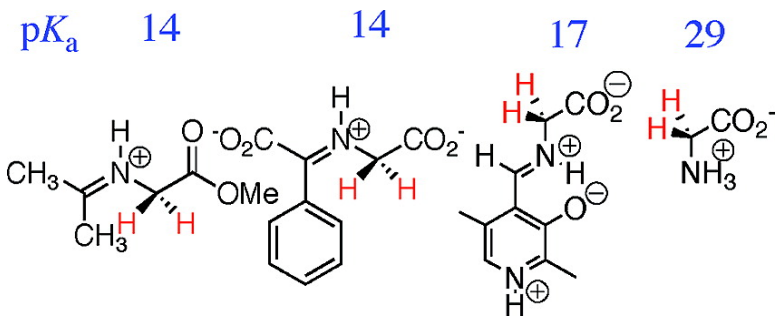

More About This Article

Additional resources and features associated with this article are available within the HTML version:

- Supporting Information
- Access to high resolution figures
- Links to articles and content related to this article
- Copyright permission to reproduce figures and/or text from this article

View the Full Text HTML

J|A|C|S
ARTICLES
Published on Web 01/17/2008

Glycine Enolates: The Effect of Formation of Iminium Ions to Simple Ketones on α-Amino Carbon Acidity and a Comparison with Pyridoxal Iminium Ions

Juan Crugeiras,[#] Ana Rios,*[,#] Enrique Riveiros,[#] Tina L. Amyes,[†] and John P. Richard*[,†]

Departamento de Química Física, Facultad de Química, Universidad de Santiago, 15782 Santiago de Compostela, Spain and Department of Chemistry, and University at Buffalo, SUNY, Buffalo, New York 14260

Received October 18, 2007; E-mail: qfarr2cn@usc.es; jrichard@chem.buffalo.edu

Abstract: Equilibrium constants in D_2O were determined by ^1H NMR analyses for formation of imines/iminium ions from addition of glycine methyl ester to acetone and from addition of glycine to phenylglyoxylate. First-order rate constants, also determined by ^1H NMR, are reported for deuterium exchange between solvent D_2O and the α-amino carbon of glycine methyl ester and glycine in the presence of increasing concentrations of ketone and Brønsted bases. These rate and equilibrium data were used to calculate second-order rate constants for deprotonation by DO^- and by Brønsted bases of the α-imino carbon of the ketone adducts. Formation of the iminium ion between acetone and glycine methyl ester and between phenylglyoxylate and glycine is estimated to cause 7 unit and 15 unit decreases, respectively, in the pK_a's of 21 and 29 for deprotonation of the parent carbon acids. The effect of formation of iminium ions to phenylglyoxylate and to 5′-deoxypyridoxal (DPL) [Toth, K.; Richard, J. P. *J. Am. Chem. Soc.* **2007**, *129*, 3013−3021] on the carbon acidity of glycine is similar. However, DPL is a much better catalyst than phenylglyoxylate of deprotonation of glycine, because of the exceptionally large thermodynamic driving force for conversion of the amino acid and DPL to the reactive iminium ion.

1. Introduction

We are interested in characterizing the kinetic and thermodynamic barriers for deprotonation of the α-amino carbon of amino acids[1−3] and peptides[4] in water and in understanding the mechanism by which enzymes lower these barriers in catalysis of deprotonation of amino acids.[1,5] There are enzymes which catalyze deprotonation of amino acids such as alanine,[6,7] glutamate,[8−10] and diaminopimelate[11] without any assistance from an electrophilic cofactor to stabilize negative charge at the α-amino carbon. The results of experimental,[1,5,12,13] computational,[10] and X-ray crystallographic studies[11] are converging to show that the conversion of the protein-bound amino acid to the zwitterionic carbanion reaction intermediate is strongly favored by catalysis at a nonpolar enzyme active site.[5]

Pyridoxal 5′-phosphate (PLP) is an extraordinary electrophilic catalyst of carbon deprotonation of α-amino acids in water,[14,15] and at enzyme active sites.[16] The first step in the mechanism for covalent catalysis by PLP is formation of an imine between the amino acid and PLP. Formation of this adduct labilizes all of the bonds of the α-imino carbon, because heterolytic bond cleavage with loss of H^+, CO_2, or R^+ gives a carbanion that is strongly stabilized by delocalization of negative charge onto the pyridine ring of the cofactor.

The presence of the pyruvoyl prosthetic group at enzymes that catalyze decarboxylation of amino acids suggests that this ketone is an effective electrophilic catalyst of reactions that proceed through α-amino carbanion intermediates.[17−20] How-

[#] Universidad de Santiago.
[†] University at Buffalo, SUNY.

(1) Rios, A.; Amyes, T. L.; Richard, J. P. *J. Am. Chem. Soc.* **2000**, *122*, 9373−9385.
(2) Rios, A.; Crugeiras, J.; Amyes, T. L.; Richard, J. P. *J. Am. Chem. Soc.* **2001**, *123*, 7949−7950.
(3) Rios, A.; Richard, J. P. *J. Am. Chem. Soc.* **1997**, *119*, 8375−8376.
(4) Rios, A.; Richard, J. P.; Amyes, T. L. *J. Am. Chem. Soc.* **2002**, *124*, 8251−8259.
(5) Richard, J. P.; Amyes, T. L. *Bioorg. Chem.* **2004**, *32*, 354−366.
(6) Spies, M. A.; Toney, M. D. *Biochemistry* **2003**, *42*, 5099−5107.
(7) Spies, M. A.; Woodward, J. J.; Watnik, M. R.; Toney, M. D. *J. Am. Chem. Soc.* **2004**, *126*, 7464−7475.
(8) Gallo, K. A.; Tanner, M. E.; Knowles, J. R. *Biochemistry* **1993**, *32*, 3991−3997.
(9) Glavas, S.; Tanner, M. E. *Biochemistry* **1999**, *38*, 4106−4113.
(10) Puig, E.; Garcia-Viloca, M.; Gonzalez-Lafont, A.; Lluch, J. M. *J. Phys. Chem. A* **2006**, *110*, 717−725.
(11) Pillai, B.; Cherney, M. M.; Diaper, C. M.; Sutherland, A.; Blanchard, J. S.; Vederas, J. C.; James, M. N. G. *Proc. Nat. Acad. Sci. U.S.A.* **2006**, *103*, 8668−8673.
(12) Patrick, J. S.; Yang, S. S.; Cooks, R. G. *J. Am. Chem. Soc.* **1966**, *118*, 231−232.
(13) Price, W. D.; Jockusch, R. A.; Williams, E. R. *J. Am. Chem. Soc.* **1998**, *120*, 3474−3484.
(14) Dixon, J. E.; Bruice, T. C. *Biochemistry* **1973**, *12*, 4762−4766.
(15) Toth, K.; Richard, J. P. *J. Am. Chem. Soc.* **2007**, *129*, 3013−3021.
(16) Toney, M. D. *Arch. Biochem. Biophys.* **2005**, *433*, 279−287.
(17) Tolbert, W. D.; Zhang, Y.; Cottet, S. E.; Bennett, E. M.; Ekstrom, J. L.; Pegg, A. E.; Ealick, S. E. *Biochemistry* **2003**, *42*, 2386−2395.
(18) Graham, D. E.; Xu, H.; White, R. H. *J. Biol. Chem.* **2002**, *277*, 23500−23507.
(19) Bach, R. D.; Canepa, C. *J. Am. Chem. Soc.* **1997**, *119*, 11725−11733.
(20) Gallagher, T.; Rozwarski, D. A.; Ernst, S. R.; Hackert, M. L. *J. Mol. Biol.* **1993**, *230*, 516−528.

10.1021/ja078006c CCC: $40.75

Chart 1

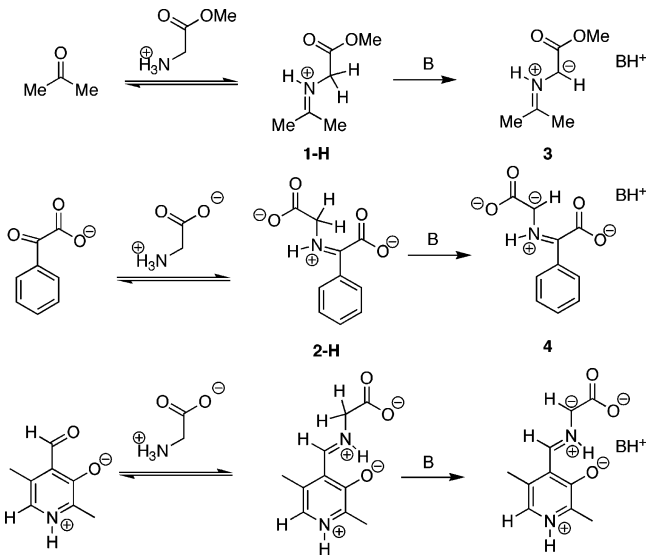

ever, there is little known about the relative advantage for electrophilic catalysis of deprotonation of amino acids by simple carbonyl compounds and by PLP, because there have been few model studies of such catalysis by the former electrophiles.[21,22] We have reported that the simple ketone acetone possesses a significant fraction of the power of PLP as a catalyst of the deprotonation of amino acids, because of the strong carbon acidity of the iminium ion adduct **1-H** (Chart 1).[2] We report here the full results from our earlier communication and extensive new data for Brønsted base catalysis of deprotonation of **1-H** and for catalysis of deprotonation of glycine by phenylglyoxylate (Chart 1). A comparison of data for catalysis of the deprotonation of glycine by phenylglyoxylate and for catalysis by 5′-deoxypyridoxal (DPL)[15] shows that the α-amino carbon acidity of adducts to phenylglyoxylate (**2-H**, Chart 1) and to DPL are similar. In other words, the problem of increasing the acidity of the α-amino carbon of amino acids may be solved by formation of iminium ion adducts to carbonyl compounds with structures much simpler than that for PLP. On the other hand, we find that DPL is a much better catalyst of carbon deprotonation than phenylglyoxylate at pD 7, so that there are other properties of PLP, which confer upon it a unique role as a cofactor in catalysis of bioorganic reactions.

2. Experimental Section

2.1. Materials. Deuterium chloride (37 wt %, 99.5% D), potassium deuterioxide (40 wt %, 98 + % D), deuterium oxide (99.9% D), acetone-d_6 (99.9 atom % D), glycine methyl ester hydrochloride, quinuclidine hydrochloride, 3-quinuclidinol, 3-chloroquinuclidine hydrochloride, 1,1,1,3,3,3-hexafluoro-2-propanol (HFIP), and 2,2,2-trifluoroethanol (TFE) were from Aldrich. Glycine and phenylglyoxylic acid were purchased from Fluka. The 3-substituted quinuclidines were purified by recrystallization from the following solvents: quinuclidine hydrochloride, ethanol; 3-quinuclidinol, acetone and 3-chloroquinuclidine hydrochloride, 1:1 (v:v) methanol/propanol. All other chemicals were reagent grade and were used without further purification.

2.2. General Methods. The acidic protons of glycine, glycine methyl ester hydrochloride, K_2HPO_4, KH_2PO_4, the hydrochlorides of quinuclidine and 3-chloroquinuclidine and the hydroxyl proton of 3-quinuclidinol were exchanged for deuterium, as described previously, before preparing solutions in D_2O.[1,4] Phenylglyoxylic acid, methoxyacetic acid, HFIP, and TFE were dissolved directly in D_2O, which resulted in <1 atom % increases in the protium content of this solvent. Phosphate buffers were prepared by mixing stock solutions of K_2DPO_4 and KD_2PO_4 in D_2O at $I = 1.0$ (KCl) to give the desired acid/base ratio. Acetate buffers were prepared by dissolving the basic form of the buffer in D_2O that contains KCl followed by addition of DCl to give the desired acid/base ratio at $I = 1.0$ (KCl). Buffers of methoxyacetate, HFIP, and TFE were prepared by dissolving their acidic forms and KCl in D_2O followed by addition of KOD to give the desired acid/base ratio at $I = 1.0$ (KCl). Solutions of quinuclidine, 3-quinuclidinol, and 3-chloroquinuclidine cations in phosphate buffer at pD = 7.6 were prepared by mixing the tertiary ammonium ion ($I = 1.0$, KCl) and phosphate buffer ($I = 1.0$, KCl) and 1 M KCl to give 0.1 M buffer.

The pH and pD were determined at 25 °C using an Orion model 720A pH meter equipped with a Radiometer GK2321C combination electrode ($\gamma_{OL} = 0.79$) or an Orion model 350 pH meter equipped with a Radiometer pHC4006-9 electrode ($\gamma_{OL} = 0.78$). Values of pD were obtained by adding 0.4 to the observed pH meter reading.[23] The concentration of deuterioxide ion at any pD was calculated using eq 1, where $K_w = 10^{-14.87}$ is the ion product of deuterium oxide at 25 °C and γ_{OL} is the apparent activity coefficient of DO^- under our experimental conditions.[24,25]

$$[DO^-] = \frac{10^{pD-pK_w}}{\gamma_{OL}} \quad (1)$$

2.3. ^{1}H NMR Analyses. ^{1}H NMR spectra at 500 MHz were recorded in D_2O on a Varian Unity Inova 500 NMR spectrometer or a Bruker AMX500 NMR spectrometer as described in previous work.[1,24,26,27] In all cases, the relaxation delay between pulses was at least 10-fold longer than the longest relaxation time of the protons of the substrates being examined ($T_1 = 4$ s for glycine methyl ester and glycine). Spectra were obtained with a sweep width of 2600 Hz, a 90° pulse angle, and an acquisition time of 6 s. Baselines were corrected for drift before integration of the peaks. Chemical shifts are reported relative to HOD at 4.67 ppm or $(CH_3)_4N^+$ at 2.94 ppm.

2.4. Determination of Equilibrium Constants. The position of the equilibrium for formation of imines to glycine and glycine methyl ester was determined by ^{1}H NMR analysis at 25 °C. The formation of the imine of glycine methyl ester was monitored in solutions that contained 0.1 M glycine methyl ester and 3.0 M acetone at $I = 1.0$ (KCl). The formation of the imine of glycine was monitored in solutions that contained 0.1−2.0 M glycine, 0.8 M phenylglyoxylate at $I = 1.0$ (KCl). The pD was maintained by use of 0.10 M of the following buffers: methoxyacetic acid, pD 3.3−4.8; acetic acid, pD 4.5−6; phosphate, pD 6.2−8; HFIP, pD 8.9, and TFE, pD 12−13. Glycine methyl ester served as the buffer for experiments at pD > 8. Hydrolysis of the ester at pD < 8.8 was not significant (<6%) during the ca. 1 h time needed to record NMR spectra, but the breakdown of the ester at higher pD prevented the determination of equilibrium constants for imine/iminium ion formation.

$$(K_{add})_{obsd} = \frac{[\mathbf{X} - \mathbf{D}]_T}{[Gly]_T[Ketone]} = \frac{A_{CH_2}^{\mathbf{X-D}}}{A_{CH_2}^{Gly}[Ketone]} \quad \mathbf{X} = 1, 2 \quad (2)$$

(21) Owen, T. C.; Young, P. R., Jr. *FEBS Lett.* **1974**, *43*, 308−312.
(22) Young, P. R.; Howell, L. G.; Owen, T. C. *J. Am. Chem. Soc.* **1975**, *97*, 6544−6551.
(23) Glasoe, P. K.; Long, F. A. *J. Phys. Chem.* **1960**, *64*, 188−190.
(24) Amyes, T. L.; Richard, J. P. *J. Am. Chem. Soc.* **1996**, *118*, 3129−3141.
(25) Rios, A.; O'Donoghue, A. C.; Amyes, T. L.; Richard, J. P. *Can. J. Chem.* **2005**, *83*, 1536−1542.
(26) Richard, J. P.; Williams, G.; Gao, J. *J. Am. Chem. Soc.* **1999**, *121*, 715−726.
(27) Amyes, T. L.; Richard, J. P. *J. Am. Chem. Soc.* **1992**, *114*, 10297−10302.

Scheme 1

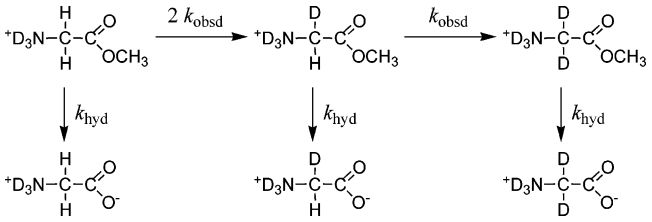

Values of the observed equilibrium constant $(K_{add})_{obsd}$ (M^{-1}) for imine formation were determined from the ratio of the integrated areas of the peaks for the methylene protons of the imine product ($A^{X-D}_{CH_2}$), and of the reactant glycine or glycine methyl ester ($A^{Gly}_{CH_2}$, eq 2). The relative equilibrium concentration of the glycine−phenylglyoxylate imine at pD > 8 was determined 24 h after mixing the reactants in order to ensure that chemical equilibrium had been reached. The rate of phenylglyoxylate-catalyzed exchange of the α-CH_2 hydrogen of glycine for solvent deuterium at pD 12−13 is similar to the rate of imine formation. However, ^{1}H NMR analysis shows that deuterium enrichment of the α-CH_2 groups of glycine and of the phenylglyoxylate imine are the same within experimental error. Therefore, there is no detectable enrichment of either species with deuterium, and the ratio of the concentrations of glycine and its imine to phenylglyoxylate anion may be determined as the ratio of the sum of integrated peak areas for the −CH_2− and −CHD− groups from ^{1}H NMR analyses.

2.5. Kinetic Measurements. All deuterium-exchange reactions were carried out in D_2O at 25 °C and I = 1.0 (KCl). The reactions were initiated by preparing solutions of the carbon acid, ketone catalyst, and the buffer at the same pD and I = 1.0 (KCl) and mixing these reagents to give a final carbon acid concentration of 15 mM. A slow downward drift in the pD was observed during the deuterium exchange reactions of glycine methyl ester, due to the competing hydrolysis of the ester.[2] The pD of these solutions was monitored and maintained within 0.05 unit of the initial value by the addition of an aliquot of a 2 M KOD solution. An even slower increase (0.03 units in two weeks) in pD was observed during deuterium exchange of glycine catalyzed by phenylglyoxylate in the presence of lowest concentrations of buffer. No new major signals were detected by ^{1}H NMR, and no significant deviation was observed in the kinetic plots of data for this reaction.

The exchange for deuterium of the first α-H of glycine and of glycine methyl ester was followed by monitoring the disappearance of the singlet due to the −CH_2− group of the substrate and the appearance of the upfield-shifted triplet due to the −CHD− group by ^{1}H NMR spectroscopy at 500 MHz, as described in previous work.[2] Reactions were monitored during the exchange for deuterium of 20−90% of the first α-H of the substrate, and the reaction progress, R, was calculated using eq 3, where A_{CH_2} and A_{CHD} are the integrated areas of the peaks for the α-CH_2 and the α-CHD groups, respectively. Observed first-order rate constants for exchange for deuterium of a *single* proton of the α-CH_2 group of the substrate, k_{obsd} (s^{-1}), were determined from the slopes of linear semilogarithmic plots of R against time (eq 4). The values of the first-order rate constant for exchange of the first α-CH_2 proton to give monodeuterated product, k_{ex} (s^{-1}), were determined as $k_{ex} = 2\ k_{obsd}$.[2]

$$R = \frac{A_{CH_2}}{A_{CH_2} + A_{CHD}} \tag{3}$$

$$\ln R = -k_{obsd}t \tag{4}$$

The rates of the deuterium exchange and hydrolysis reactions of glycine methyl ester in the presence of acetone are similar at pD 7.6. The deuterium enrichment of the glycine product of the hydrolysis reaction was determined by ^{1}H NMR analysis after more than 10 halftimes for the hydrolysis reaction. The values of $k_{ex} = 2k_{obsd}$ (Scheme 1) were determined from the integrated areas of the singlet due to the α-CH_2 group of glycine and the triplet due to the α-CHD group of glycine using eq 5, where k_{hyd} is the first-order rate constant for hydrolysis of glycine methyl ester under the conditions of the experiment. The values of k_{hyd} were calculated from eq 6, where $f_{ND_3^+}$ is the fraction of substrate present in the reactive N-protonated form, and using the second-order rate constants $(k_B)_{hyd}$ for general base catalysis of the hydrolysis reaction (Table S1 of the Supporting Information) calculated from data reported in part in earlier work.[2] A control experiment at pD 6.6 showed that there is no change in k_{hyd} (±5%), for reaction in the presence of a fixed concentration of phosphate buffer, as the concentration of acetone is increased from 0 to 0.2 M. This shows that there is no significant catalysis of the hydrolysis reaction of glycine methyl ester by acetone.

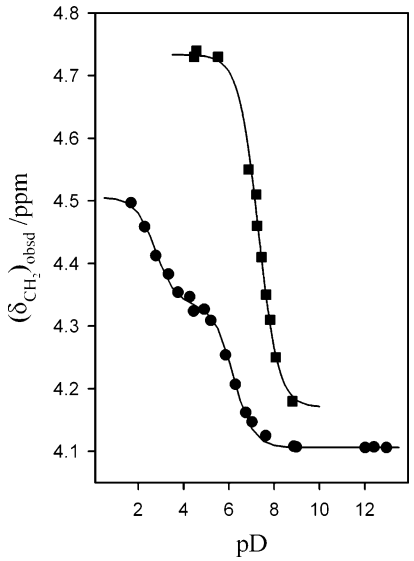

Figure 1. The dependence on pD of $(\delta_{CH_2})_{obsd}$ (ppm) for the −CH_2− hydrogen of the imine formed in D_2O that contains: (■), 0.1 M glycine methyl ester and 3 M acetone; (●), glycine (0.1−2.0 M, depending upon the pD), and 0.8 M phenylglyoxylate at 25 °C and I = 1.0 (KCl). The solid lines show the fit of the data to eq 7 derived for Scheme 2 (■), or to eq 8 derived for Scheme 3 (●).

$$k_{ex} = \frac{k_{hyd}}{\left(\frac{A_{CH_2}}{2A_{CHD}} - \frac{1}{2}\right)} \tag{5}$$

$$k_{hyd} = \sum((k_B)_{hyd}[B])f_{N_{D^+_3}} \tag{6}$$

3. Results

3.1. Equilibrium Constants for Imine Formation. Figure 1 (■) shows the change with changing pD in $(\delta_{CH_2})^{\mathbf{1}}_{obsd}$ (ppm) of the signal for the α-CH_2 group of **1/1-D** (Scheme 2) that forms in D_2O that initially contains 0.1 M glycine methyl ester and 3 M acetone at 25 °C and I = 1.0 (KCl). The signal for the α-CH_2 group moves from 4.18 ppm at pD 8.8 to 4.73 ppm at pD 4.5, because of protonation of the imino nitrogen. The solid line in Figure 1 shows the nonlinear least-squares fit of the data to eq 7, derived for Scheme 2, where (a) $\delta^{\mathbf{1-D}}_{CH_2} = 4.73$ and $\delta^{\mathbf{1}}_{CH_2} = 4.18$ ppm are the chemical shifts of the α-CH_2 group observed at extreme low and high pD, and (b) $(K_a)_{\mathbf{1-D}} = 10^{-7.3}$ is determined by treating this acidity constant as a variable parameter (Scheme 2).

Scheme 2

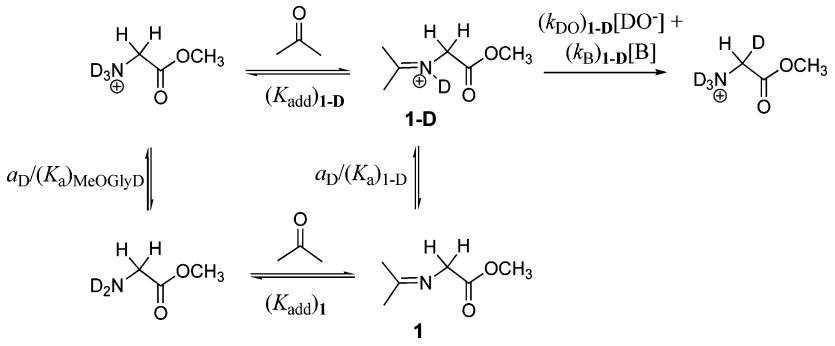

Scheme 3

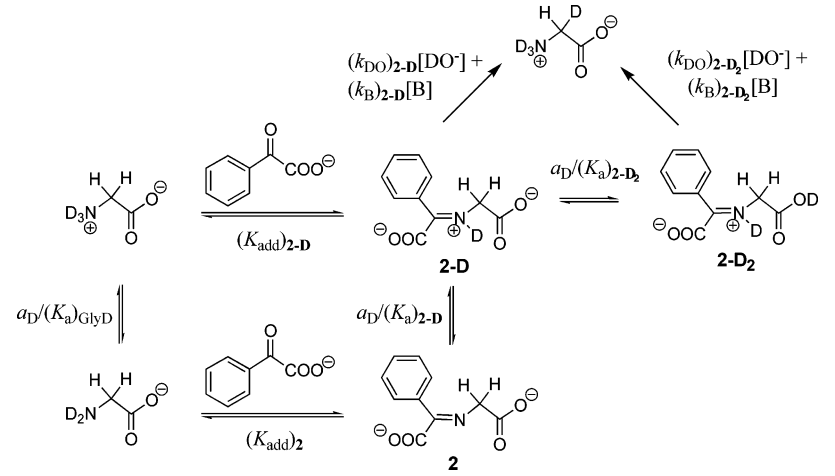

Table 1. Equilibrium Constants in D_2O for Addition of Glycine Methyl Ester to Acetone (Scheme 2) and for Addition of Glycine to Phenylglyoxylate (Scheme 3)[a]

ketone	amino compound	imine	$p(K_a)_{Gly}$ [b]	$p(K_a)_{X-D}$ [c]	K_{add} [d]/M^{-1}
$(CH_3)_2CO$ [e]	$^+D_3NCH_2COOCH_3$	**1-D**	8.48	7.30 ± 0.04	$(3.3 \pm 0.4) \times 10^{-3}$
	$D_2NCH_2COOCH_3$	**1**			$(5.0 \pm 0.8) \times 10^{-2}$
$C_6H_5COCOO^-$ [f]	$^+D_3NCH_2COOD$	**2-D$_2$**		2.76 ± 0.09	
	$^+D_3NCH_2COO^-$	**2-D**	10.35	6.19 ± 0.04	$(1.0 \pm 0.1) \times 10^{-4}$
	$D_2NCH_2COO^-$	**2**			1.50 ± 0.01

[a] At 25 °C and $I = 1.0$ (KCl). [b] The acidity constant of the amino acid in D_2O at 25 °C and $I = 1.0$ (KCl) determined by potentiometric titration.[1] [c] Apparent acidity constants in D_2O at 25 °C and $I = 1.0$ (KCl), determined by NMR titration as described in the text. [d] Equilibrium constant for the addition of the amino acid to the corresponding carbonyl compound. [e] Equilibrium constants defined by Scheme 2. [f] Equilibrium constants defined by Scheme 3.

Figure 1 (●) also shows the change with changing pD in $(\delta_{CH_2})^{\mathbf{2}}_{obsd}$ (ppm) of the signal for the α-CH_2 group of **2**/**2-D**/**2-D$_2$** (Scheme 3) that forms in D_2O that initially contains glycine (0.1−2.0 M depending upon the pD) and 0.8 M phenylglyoxylate at 25 °C and $I = 1.0$ (KCl).[28] The chemical shift of the α-CH_2 group changes because of protonation of the imine nitrogen and of the amino acid carboxylate groups. The solid line shows the fit of these data to eq 8, derived for Scheme 3, where $\delta^{\mathbf{2-D_2}}_{CH_2} = 4.51$, $\delta^{\mathbf{2-D}}_{CH_2} = 4.33$, and $\delta^{\mathbf{2}}_{CH_2} = 4.11$ ppm are the ^1H NMR chemical shifts for the $-CH_2-$ group of the different ionic forms of **2**, and $(K_a)_{\mathbf{2-D_2}}$ and $(K_a)_{\mathbf{2-D}}$ are the acidity constants for **2-D$_2$** and **2-D** (Table 1) determined from the nonlinear least-squares fit of the experimental data to eq 8. There is a relatively large uncertainty in the value of $(K_a)_{\mathbf{2-D_2}}$ because of the limited data for imine formation at low pD (Figure 2). Scheme 3 shows protonation of the glycine carboxylate of **2-D**, for the sake of simplicity. However, there are insufficient data to distinguish this from protonation of the α-imino carboxylate.

$$(\delta_{CH_2})^{\mathbf{1}}_{obsd} = \frac{\delta^{\mathbf{1}}_{CH_2}(K_a)_{\mathbf{1-D}} + \delta^{\mathbf{1-D}}_{CH_2} a_D}{((K_a)_{\mathbf{1-D}} + a_D)} \quad (7)$$

$$(\delta_{CH_2})^{\mathbf{2}}_{obsd} = \frac{\delta^{\mathbf{2}}_{CH_2}(K_a)_{\mathbf{2-D}}(K_a)_{\mathbf{2-D_2}} + \delta^{\mathbf{2-D}}_{CH_2}(K_a)_{\mathbf{2-D_2}} a_D + \delta^{\mathbf{2-D_2}}_{CH_2} a_D^2}{((K_a)_{\mathbf{2-D}}(K_a)_{\mathbf{2-D_2}} + (K_a)_{\mathbf{2-D_2}} a_D + a_D^2)} \quad (8)$$

$$(K_{add})_{obsd} = (K_{add})_{\mathbf{X-D}}\left(\frac{a_D + (K_a)_{\mathbf{X-D}}}{a_D + (K_a)_{GlyD}}\right) \quad (9)$$

The apparent equilibrium constants $(K_{add})_{obsd}$ (M^{-1}) for addition of glycine methyl ester to acetone, or for addition of glycine to phenylglyoxylate, to form the corresponding imines

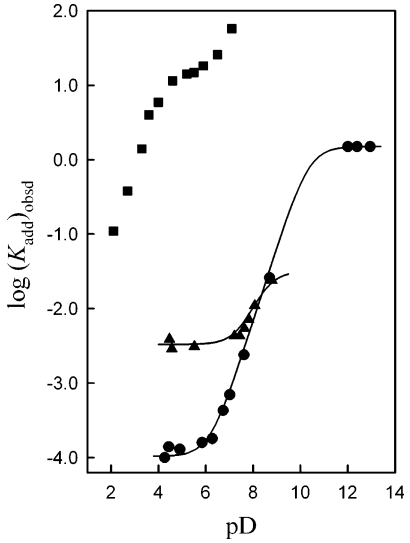

Figure 2. Logarithmic dependence of $(K_{add})_{obsd}$ (M^{-1}) on pD for conversion of glycine and glycine methyl ester to the corresponding imines in D_2O at 25 °C and $I = 1.0$ (KCl). (Key) Reaction of glycine with phenylglyoxylate (●). The solid line was calculated using eq 9 (X = **2**) and the equilibrium constants from Table 1. Reaction of glycine methyl ester with acetone (▲). The solid line was calculated using eq 9 (X = **1**) and the equilibrium constants from Table 1. Reaction of glycine with 5′-deoxypyridoxal in H_2O (■).[15]

in D_2O at 25 °C were determined by ^1H NMR analysis as described in the Experimental Section. Figure 2 shows the change, with changing pD, in $\log(K_{add})_{obsd}$ for addition of glycine methyl ester to acetone (▲) or of glycine to phenylglyoxylate (●). The line through the triangles shows the fit of data for the first reaction to eq 9 (**X** = 1), derived for Scheme 2, using $(K_a)_{MeOGlyD} = 3.3 \times 10^{-9}$ M,[1] $(K_a)_{\mathbf{1-D}} = 5.0 \times 10^{-8}$ M (Table 1) and $(K_{add})_{\mathbf{1-D}} = 0.0033$ M^{-1} determined for the formation of the iminium ion at low pD. The line through the circles in Figure 2 shows the fit of data for the second reaction to eq 9 (**X** = 2), derived for Scheme 3, using $(K_a)_{GlyD} = 4.5 \times 10^{-11}$ M,[1] $(K_a)_{\mathbf{2-D}} = 6.5 \times 10^{-7}$ M (Table 1) and values of $(K_{add})_{\mathbf{2}} = 1.50$ M^{-1} and $(K_{add})_{\mathbf{2-D}} = (1.0 \pm 0.1) \times 10^{-4}$ M^{-1} determined for the reaction at low and high pD, respectively. Figure 2 (■) also shows values of $(K_{add})_{obsd}$ for addition of glycine to 5′-deoxypyridoxal determined in earlier work.[15]

3.2. Rate Constants for Deuterium Exchange. 3.2.1. Catalysis by Acetone. The exchange for deuterium of the first α-proton of the methylene group of glycine methyl ester in D_2O at 25 °C and $I = 1.0$ (KCl) was followed by ^1H NMR (500 MHz) as described in previous work.[1,4] Figure 3A shows the linear dependence of $k_{ex} = 2k_{obsd}$ (Scheme 1) on the total concentration of acetate buffer (pD 5.56) for reactions in the presence of increasing [acetone]. The intercepts of these correlations are equal to $k_o = k_w f_{\mathbf{1-D}}$ (s^{-1}, Table 2) for deuterium exchange catalyzed by the solvent, where $f_{\mathbf{1-D}}$ is the fraction of glycine methyl ester present as the iminium ion adduct **1-D** (eq 10, **X** =1, derived for Scheme 2)[29] and k_w is the apparent first-order rate constant for the solvent reaction.

The plot of k_o (s^{-1}, Table 2) against [acetone] shown in Figure 3B is linear. The slope is equal to the apparent rate constant

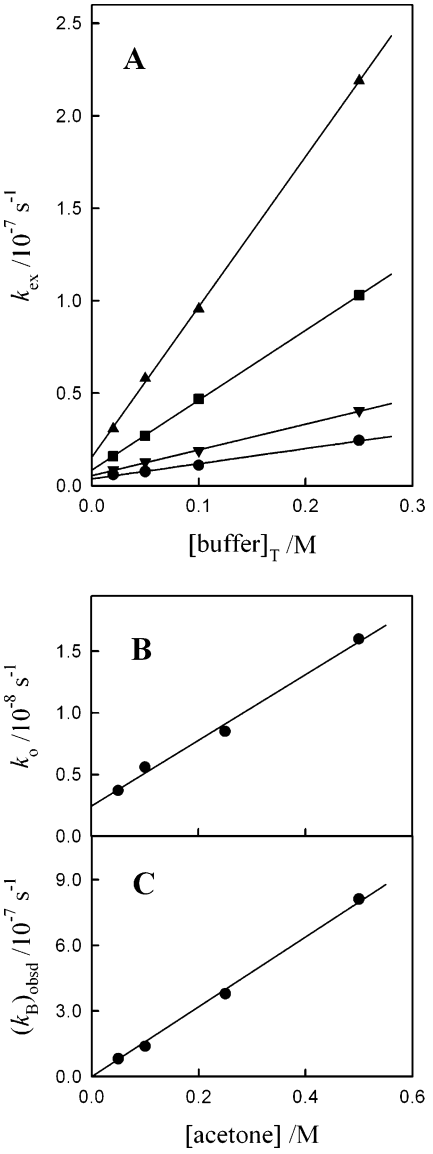

Figure 3. (A) Dependence of k_{ex} (s^{-1}) for exchange of the first α-proton of glycine methyl ester in the presence of acetone on the total concentration of acetate buffer (pD = 5.56) in D_2O at 25 °C and $I = 1.0$ (KCl). (Key) (●) 0.05 M acetone; (▼) 0.10 M; (■) 0.25 M; (▲) 0.50 M. (B) Dependence of the intercepts of the linear correlations in Figure 3A (k_o) on [acetone]. The slope of Figure 3B gives $(k_w)_{obsd}$ (M^{-1} s^{-1}) for the acetone-catalyzed deuterium exchange reaction at pD 5.56. (C) Dependence of the slopes of the linear correlations in Figure 3A $(k_B)_{obsd}$ on [acetone]. The slope gives $(k_B^T)_{obsd}$ (M^{-2} s^{-1}) for a termolecular acetone and buffer-catalyzed deuterium exchange reaction at pD 5.56.

$(k_w)_{obsd} = 2.7 \times 10^{-8}$ M^{-1} s^{-1} for acetone-catalyzed deprotonation of glycine methyl ester by solvent at pD 5.56 (eq 11). Equation 12, which can be simply derived from eq 10 and 11, shows the relationship between $(k_w)_{obsd}$ and k_w for deprotonation of **1-D** by the solvent D_2O. Substitution of $(k_w)_{obsd} = 2.7 \times 10^{-8}$ $M^{-1}s^{-1}$, $(K_{add})_{\mathbf{1-D}} = 0.0033$ M^{-1}, $(K_a)_{Gly-D} = 3.3 \times 10^{-9}$ M and $a_D = 10^{-5.56}$ M into eq 12 gives $k_w = 8.2 \times 10^{-6}$ s^{-1}. The same analysis of data for reactions in phosphate buffers at pD 7.64 and 6.61 (Table 2) gives $k_w = 9.3 \times 10^{-4}$ s^{-1} and $k_w = 1.0 \times 10^{-4}$ s^{-1}, respectively. Figure 4 (●) shows the pD-rate profile of log k_w for deprotonation of **1-D** in D_2O. The

(28) There is little hydration of the carbonyl group of phenylglyoxalate (≪1%) because only 5% of pyruvate anion is hydrated in water [Esposito, A.; Lukas, A.; Meany, J. E.; Pocker, Y. *Can. J. Chem.* **1999**, *77*, 1108−1117] and the phenyl for methyl group substitution at pyuvate is expected to cause the same ca. 130-fold decrease in the equilibrium constant for hydration observed for acetaldehyde [Guthrie, J. P. *J. Am. Chem. Soc.* **2000**, *122*, 5529−5538].

(29) Derived by assuming that the concentration of imine/iminium ion is negligible because less than 1% of the amino acid is converted to the imine/iminium ion adduct in the presence of 0.5 M acetone at pD < 8.

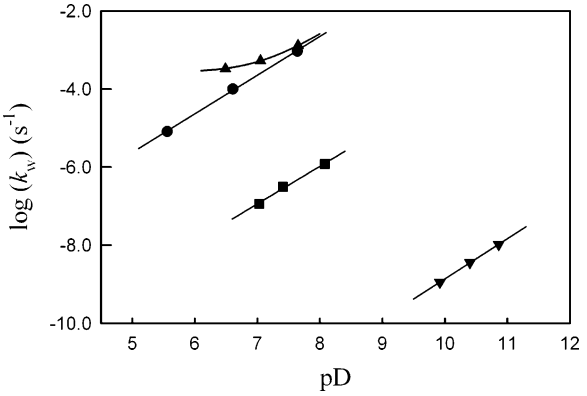

Figure 4. pD-rate profiles of k_w (s^{-1}) for exchange for deuterium of: (a) (●), the first α-CH_2− hydrogen of **1-D**; (b) (▲), the first α-CH_2− hydrogen of **2-D**. (c) (■), the first α-CH_2− hydrogen of N-protonated glycine methyl ester;[1] (▼), the first α-CH_2− hydrogen of N-protonated glycine.[1]

Table 2. Rate Constants for Exchange of the First α-Proton of Glycine Methyl Ester in the Presence of Acetone and Phosphate or Acetate Buffers in D_2O[a]

base	pD	[acetone] / M	k_o / s^{-1} [c]	$(k_B)_{obsd}$ / $M^{-1}s^{-1}$ [d]	$(k_w)_{obsd}$ / $M^{-1}s^{-1}$ [e]	$(k_B^T)_{obsd}$ / $M^{-2}s^{-1}$ [f]
DPO_4^{2-} $pK_{BD} = 7.0$[b]	7.64	0.01	3.7×10^{-7}	2.9×10^{-6}	2.7×10^{-6}	1.1×10^{-4}
		0.02	4.1×10^{-7}	3.9×10^{-6}		
		0.05	4.9×10^{-7}	7.4×10^{-6}		
		0.10	6.2×10^{-7}	1.3×10^{-5}		
	6.61	0.02	4.7×10^{-8}	1.1×10^{-6}	3.3×10^{-7}	4.5×10^{-5}
		0.05	6.3×10^{-8}	2.3×10^{-6}		
		0.10	8.0×10^{-8}	4.1×10^{-6}		
		0.20	1.1×10^{-7}	9.1×10^{-6}		
CH_3COO^- $pK_{BD} = 5.0$[b]	5.56	0.05	3.7×10^{-9}	8.2×10^{-8}	2.7×10^{-8}	1.6×10^{-6}
		0.10	5.6×10^{-9}	1.4×10^{-7}		
		0.25	8.5×10^{-9}	3.8×10^{-7}		
		0.50	1.6×10^{-8}	8.1×10^{-7}		

[a] At 25 °C and $I = 1.0$ (KCl). [b] Apparent pK_a's of the conjugate acids in D_2O at 25 °C and $I = 1.0$ (KCl).[24] [c] Apparent first-order rate constants for deuterium exchange, determined as the intercepts of plots of k_{ex} (s^{-1}) against $[buffer]_T$. [d] Apparent second-order rate constants for buffer-catalyzed deuterium exchange, determined as the slopes of plots of k_{ex} (s^{-1}) against $[buffer]_T$. [e] Apparent second-order rate constants for acetone-catalyzed deprotonation of glycine methyl ester determined as the slopes of plots of k_o against [acetone]. [f] Observed third-order rate constants for buffer-catalyzed deprotonation of glycine methyl ester, determined as the slopes of plots of $(k_B)_{obsd}$ against [acetone].

solid line of unit slope shows that deprotonation of **1-D** is by DO^- ($(k_{DO})_{\mathbf{1-D}}$, Scheme 2). The nonlinear least-squares fit of the data to eq 13, where $K_w = 10^{-14.87}$ M^2 is the ion product of D_2O at 25 °C, and $\gamma_{OL} = 0.79$ is the apparent activity coefficient of DO^- under our experimental conditions, gives $(k_{DO})_{\mathbf{1-D}} =$ 13,000 M^{-1} s^{-1} for deprotonation of **1-D** by DO^- (Scheme 2).[2]

$$f_{\mathbf{X-D}} = \frac{(K_{add})_{\mathbf{X-D}}[\text{Ketone}]}{\left(1 + \frac{(K_a)_{\text{Gly-D}}}{a_D}\right)} \quad (10)$$

$$k_o = (k_w)_{obsd}[\text{Ketone}] = k_w f_{\mathbf{X-D}} \quad (11)$$

$$k_w = \frac{(k_w)_{obsd}\left(1 + \frac{(K_a)_{\text{Gly-D}}}{a_D}\right)}{(K_{add})_{\mathbf{X-D}}} \quad (12)$$

$$\log k_w = \log\left(\frac{(k_{DO})_{\mathbf{1-D}}K_w}{\gamma_{OL}}\right) + \text{pD} \quad (13)$$

The slopes of the correlations in Figure 3A are equal to $(k_B)_{obsd} = (k_B)_{\mathbf{1-D}} f_B f_{\mathbf{1-D}}$ (Table 2) for the deuterium exchange

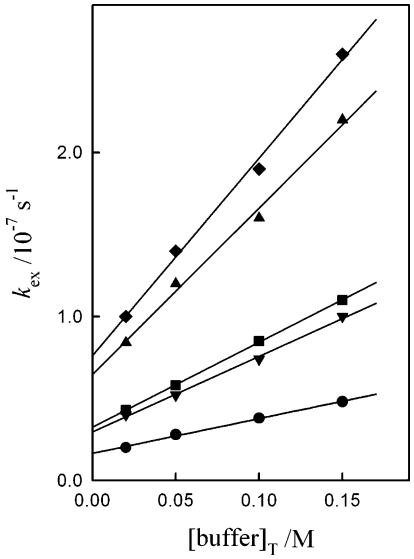

Figure 5. Dependence of k_{ex} (s^{-1}) for exchange for deuterium of the first α-proton of glycine in the presence of phenylglyoxylate on the total concentration of phosphate buffer at pD = 7.65 in D_2O at 25 °C and $I =$ 1.0 (KCl). Key: (●), 0.1 M phenylglyoxylate; (▼), 0.20 M; (■), 0.25 M; (▲), 0.40 M; (◆), 0.50 M.

reaction catalyzed by buffer at the given concentration of acetone, where $(k_B)_{\mathbf{1-D}}$ (M^{-1} s^{-1}) is the second-order rate constant for deprotonation of **1-D** by the buffer base and f_B is the fraction of the catalyst in the basic form. The values of $(k_B)_{obsd}$ increase linearly with [acetone], as shown in Figure 3C. The slope of this correlation is the apparent third-order rate constant for deprotonation of glycine methyl ester catalyzed by acetone and acetate anion, $(k_B^T)_{obsd} = 1.6 \times 10^{-6}$ M^{-2} s^{-1} (Table 2). Substitution of $(k_B^T)_{obsd}$ into eq 14 along with $(K_{add})_{\mathbf{1-D}} = 0.0033$ M^{-1}, $f_B = 0.75$, $(K_a)_{\text{Gly-D}} = 3.3 \times 10^{-9}$ M and $a_D = 10^{-5.56}$ M gives $(k_B)_{\mathbf{1-D}} = 6.5 \times 10^{-4}$ M^{-1} s^{-1} for deprotonation of **1-D** by acetate ion (Scheme 2).

$$(k_B)_{\mathbf{1-D}} = \frac{(k_B^T)_{obsd}\left(1 + \frac{(K_a)_{\text{Gly-D}}}{a_D}\right)}{f_B(K_{add})_{\mathbf{1-D}}} \quad (14)$$

A similar treatment of the data for the reactions catalyzed by phosphate buffers at pD 7.64 and 6.61 (Table 2) gives the values of $(k_B^T)_{obsd}$ reported in Table 2. Substitution of these values of $(k_B^T)_{obsd}$ into eq 14, as described above for the reactions catalyzed by acetate ion, gives values of $(k_B)_{\mathbf{1-D}} = 4.7 \times 10^{-2}$ and 4.8×10^{-2} M^{-1} s^{-1} for reactions at pD 7.64 and 6.61, respectively, for deprotonation of **1-D** by phosphate dianion.

Values of k_{ex} (s^{-1}) for the exchange for deuterium of the first α-proton of glycine methyl ester at pD 7.64 (0.1 M phosphate buffer) in the presence of acetone and quinuclidine, 3-quinuclidinol, or 3-chloroquinuclidine are reported in Table S2 of the Supporting Information. Table 3 reports values of $(k_B)_{obsd}$ (M^{-1} s^{-1}) for catalysis by these tertiary amines of deuterium exchange into glycine methyl ester that were determined from the slopes of linear plots (not shown) of k_{ex} against the total concentration of the acidic and basic forms of the amine. Values of $(k_B)_{\mathbf{1-D}}$ (M^{-1} s^{-1}) (Table 3) were calculated from the values of $(k_B)_{obsd}$ as described above for the acetate anion-catalyzed reaction.

Table 3. Rate Constants for Exchange of the First α-Proton of Glycine Methyl Ester in the Presence of Acetone and 3-Substituted Quinuclidines at pD 7.64[a]

base	pK_{BD} [b]	f_B [c]	[acetone]/ M	$(k_B)_{obsd}$/ $M^{-1}s^{-1}$ [d]	$(k_B^T)_{obsd}$/ $M^{-2}s^{-1}$ [e]	$(k_B)_{1-D}$/ $M^{-1}s^{-1}$ [f]
quinuclidine	12.1	3.5×10^{-5}	0.01	8.0×10^{-7}	4.6×10^{-5}	460 ± 30
			0.02	1.4×10^{-6}		
			0.05	2.4×10^{-6}		
			0.10	5.0×10^{-6}		
3-quinuclidinol	10.7	8.7×10^{-4}	0.01	1.9×10^{-6}	7.3×10^{-5}	29 ± 3
			0.02	2.3×10^{-6}		
			0.05	3.9×10^{-6}		
			0.10	8.4×10^{-6}		
3-chloroquinuclidine	9.7	8.6×10^{-3}	0.01	1.4×10^{-6}	9.0×10^{-5}	3.6 ± 0.5
			0.02	2.6×10^{-6}		
			0.05	6.5×10^{-6}		
			0.10	9.5×10^{-6}		

[a] In D_2O buffered with 0.1 M phosphate at 25 °C and $I = 1.0$ (KCl). [b] Apparent pK_a's of the 3-substituted quinuclidinium cations.[24] [c] Fraction of tertiary amine present in the basic form at pD 7.64. [d] Observed second-order rate constants for quinuclidine-catalyzed deuterium exchange at pD 7.64, determined as the slopes of plots of k_{ex} against the total concentration of quinuclidine. [e] Observed third-order rate constants for acetone-catalyzed deprotonation of glycine methyl ester by the 3-substituted quinuclidines at pD = 7.64, determined as the slope of a plot of $(k_B)_{obsd}$ against [acetone]. [f] Second-order rate constants for deprotonation of **1-D** by 3-substituted quinuclidines determined using eq 14.

Table 4. Rate Constants for Exchange of the First α-Proton of Glycine Catalyzed by Phenylglyoxylate in D_2O[a]

base	pD	[PhCOCOO$^-$]/ M	k_o/s^{-1} [d]	k_w/s^{-1} [e]	$(k_B)_{obsd}/M^{-1}s^{-1}$ [f]	$(k_B)/M^{-1}s^{-1}$ [g]
DPO_4^{2-}	7.65	0.10	1.7×10^{-8}	1.70×10^{-3}	2.1×10^{-7}	2.6×10^{-2}
		0.20	3.0×10^{-8}	1.50×10^{-3}	4.6×10^{-7}	2.9×10^{-2}
		0.25	3.3×10^{-8}	1.32×10^{-3}	5.2×10^{-7}	2.6×10^{-2}
	(f_B[c] = 0.8)	0.40	6.5×10^{-8}	1.63×10^{-3}	1.0×10^{-6}	3.1×10^{-2}
		0.50	7.6×10^{-8}	1.52×10^{-3}	1.2×10^{-6}	3.0×10^{-2}
$pK_{BD} = 7.0$ [b]			$(k_w)_{av} = (1.5 \pm 0.2) \times 10^{-3}$		$(k_B)_{av} = (2.8 \pm 0.3) \times 10^{-2}$	
	7.05	0.25	1.5×10^{-8}	6.0×10^{-4}	3.7×10^{-7}	3.0×10^{-2}
	(f_B[c] = 0.5)	0.50	3.3×10^{-8}	6.6×10^{-4}	1.0×10^{-6}	4.0×10^{-2}
			$(k_w)_{av} = 6 \times 10^{-4}$		$(k_B)_{av} = 3.5 \times 10^{-2}$	
	6.49	0.50	2.0×10^{-8}	4×10^{-4}	5.2×10^{-7}	5×10^{-2}
	(f_B[c] = 0.2)					

[a] At 25 °C and $I = 1.0$ (KCl). [b] Apparent pK_a of the conjugate acid in D_2O at 25 °C and $I = 1.0$ (KCl).[1] [c] Fraction of the buffer present in the basic form. [d] The intercept of plots of k_{ex} against $[B]_T$ (Figure 5). [e] Apparent first-order rate constants for solvent-catalyzed deprotonation of **2-D**, calculated from the values of k_o as described in the text. [f] The slope of plots of k_{ex} against $[B]_T$ (Figure 5). [g] Apparent second-order rate constants for buffer-catalyzed deprotonation of **2-D**, calculated from the values of $(k_B)_{obsd}$ as described in the text.

3.2.2. Catalysis by Phenylglyoxylate. The exchange for deuterium of the first α-proton of glycine was studied in D_2O at 25 °C and $I = 1.0$ (KCl) in solutions buffered with potassium phosphate (pD 6.49−7.65). Table S3 of the Supporting Information gives the observed first-order rate constants k_{ex} (s^{-1}) for deuterium exchange in the presence of various concentrations of phenylglyoxylate and phosphate buffer at pD 6.49, 7.05, and 7.65, determined as described in the Experimental Section. Figure 5 shows the effect of increasing concentrations of phosphate buffer at pD 7.65 on k_{ex} (s^{-1}) for reactions at different fixed concentrations of phenylglyoxylate. The intercepts of these linear plots are the first-order rate constants $k_o = k_w f_{\mathbf{2-D}}$ (s^{-1}, Table 4) for solvent-catalyzed exchange at pD 7.65, where $f_{\mathbf{2-D}} = (K_{add})_{\mathbf{2-D}}$[phenylglyoxylate] is the fraction of glycine present as **2-D** calculated using eq 10 [$\mathbf{X} = 2$, $1 \gg ((K_a)_{Gly-D}/a_D)$]. Table 4 reports values of k_w, calculated using eq 15, for reactions at different constant [phenylglyoxylate]. Less data is reported for reactions pD 7.05 and pD 6.49, because the slow deuterium exchange reactions could only be detected at high [phenylglyoxylate]. The linear plot (not shown) of k_w (s^{-1}) against [DO^-] was fit to eq 16 to give $(k_{DO})_{\mathbf{2-D}} = 1.7 \times 10^4$ M^{-1} s^{-1} for deprotonation of **2-D** by DO^- (Scheme 3) and $(k_w)_o = 3.1 \times 10^{-4}$ s^{-1} for either pD-independent deprotonation of **2-D** or the kinetically equivalent deprotonation of **2-D$_2$** by DO^- (see Discussion section).

$$k_w = k_o/f_{\mathbf{2-D}} \quad (15)$$

$$k_w = (k_w)_o + (k_{DO})_{\mathbf{2-D}}[DO^-] \quad (16)$$

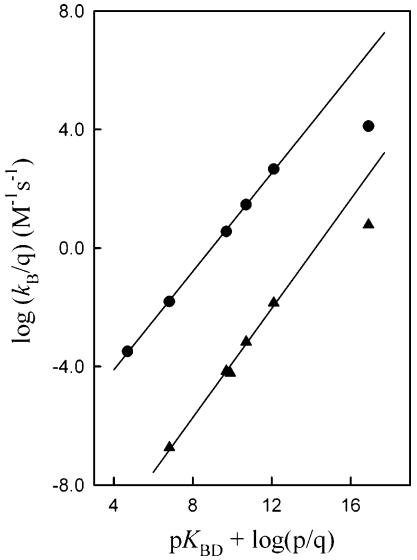

Figure 6. Statistically corrected Brønsted correlations for deprotonation of **1-D** (●) and N-protonated glycine methyl ester (▲) by buffer bases and DO^- in D_2O, where q and p are equal to the number of chemically equivalent basic sites in the reactant and equivalent acidic hydrogen in the product, respectively.

The slopes of the linear correlations in Figure 5 are apparent second-order rate constants, $(k_B)_{obsd} = k_B f_B f_{\mathbf{2-D}}$ (M^{-1} s^{-1}) for buffer-catalyzed deprotonation of glycine, where k_B is the second-order rate constant for deprotonation of **2-D** by DPO_4^{2-} (Scheme 3) and f_B is the fraction of the buffer in the basic form

Table 5. Second-Order Rate Constants for Carbon Deprotonation of **1-D**, **2-D** and **2-D$_2$** in D_2O[a]

base catalyst	pK_{BD} [b]	iminium ion	k_B/M^{-1} s^{-1} [c]
DO^-	16.6	**1-D**	$(1.3 \pm 0.1) \times 10^4$
		2-D	$(1.7 \pm 0.1) \times 10^4$
		2-D$_2$	$\sim(3.0 \pm 0.7) \times 10^8$
quinuclidine	12.1	**1-D**	460 ± 30
3-quinuclidinol	10.7	**1-D**	29 ± 3
3-chloroquinuclidine	9.7	**1-D**	3.6 ± 0.5
DPO_4^{2-}	7.0	**1-D**	$(4.7 \pm 0.2) \times 10^{-2}$
		2-D	$(2.8 \pm 0.1) \times 10^{-2}$
		2-D$_2$	$\sim(1.1 \pm 0.3) \times 10^2$
CH_3COO^-	5.0	**1-D**	$(6.5 \pm 0.2) \times 10^{-4}$

[a] At 25 °C and $I = 1.0$ (KCl). The quoted errors are standard deviations. [b] Apparent pK_a of the conjugate acid of the base catalyst in D_2O at 25 °C and $I = 1.0$ (KCl).[24] [c] Second-order rate constants for deprotonation of the iminium ion by the base catalyst, calculated from kinetic data as described in the text.

(Table 4). The values for k_B reported in Table 4 were calculated from $(k_B)_{obsd}$ using the appropriate values of f_B calculated from the pD and pK_a of the buffer catalyst, and $f_{\mathbf{2-D}} = (K_{add})_{\mathbf{2-D}}$[phenylglyoxylate] (see above). The second-order rate constants determined for deprotonation of **2-D** are also summarized in Table 5.

4. Discussion

The exchange of the α-CH_2 hydrogen of glycine methyl ester for deuterium from D_2O catalyzed by acetone was monitored at 25 °C and neutral pD, as described in earlier work.[1,4] There is no detectable (<1%) catalysis by acetone of the exchange for deuterium of the α-CH_2 hydrogen of glycine after 1-month incubation of acetone (1 M) with glycine in D_2O at pD 7.8 and 25 °C. Experiments to characterize catalysis of the exchange for deuterium of the α-CH_2 hydrogen of glycine by pyruvate, an analogue for the pyruvoyl prosthetic group used in some enzyme-catalyzed decarboxylation reactions,[17,18,20] failed because of the competing bimolecular aldol condensation reaction of pyruvate. Phenylglyoxylate was examined as a model for pyruvate that lacks acidic α-hydrogen atoms.

Reaction Pathways. The kinetic data for acetone-catalyzed deuterium exchange reactions of glycine methyl ester were fit to a mechanism in which the imine **1-D** undergoes irreversible deprotonation by DO^-, the conjugate base of solvent, and by other Brønsted bases. Two pathways are observed for deprotonation of **2-D** by solvent and buffer bases. The dominant pathway at pD 7.65 is for deprotonation of **2-D** by DO^- and phosphate dianion. The apparent rate constant for the "solvent" reaction approaches a limiting value of $k_w = 3.1 \times 10^{-4}$ s^{-1} and the apparent rate constant for the buffer-catalyzed rate constant increases as the pD is decreased to 6.49 (Table 4). These observations show that additional pathways are important for the reactions of these bases with **2** at low pD.

Figure 4 (▲) shows a logarithmic pD−rate profile of rate constants k_w for deprotonation of **2-D**. The solid line shows the fit of the data obtained using values of $(k_{DO})_{\mathbf{2-D}} = 1.7 \times 10^4$ M^{-1} s^{-1} and $(k_w)_o = 3.1 \times 10^{-4}$ s^{-1} for the DO^--catalyzed and the pD-independent reactions, respectively. No similar upward breaks at pD 5−7 are observed in the pD−rate profiles for carbon deprotonation of simpler amino acid derivatives.[1,30] This suggests that DO^- is normally so much more reactive than DOD toward deprotonation of α-amino carbon that the reaction remains first order in [DO^-] at pD 5−7. We therefore suggest that the new pathway observed at low pD is for deprotonation of a second ionic form or the substrate (**2-D$_2$**) by DO^- (Scheme 3). The observed rate constant for this reaction is pD-independent at pD > p$(K_a)_{\mathbf{2-D_2}}$ (Table 1) because the decrease in DO^- at decreasing pD is balanced by the increase in the concentration of the strong carbon acid **2-D$_2$**. Equation 17 gives the relationship between the apparent pD-independent rate constant $(k_w)_o$ and $(k_{DO})_{\mathbf{2-D_2}}$ for the deprotonation of the minor ionic form **2-D$_2$** by deuterioxide ion. A value of $(k_{DO})_{\mathbf{2-D_2}} \approx 3 \times 10^8$ M^{-1} s^{-1} (Table 5) was calculated using eq 17, the experimental value for $(k_w)_o$, $K_w = 10^{-14.87}$ M^2, $\gamma_{OL} = 0.78$ and $(K_a)_{\mathbf{2-D_2}} \approx 1.7 \times 10^{-3}$ M (Table 1).

$$(k_w)_o = \frac{(k_{DO})_{\mathbf{2-D_2}} K_w}{(K_a)_{\mathbf{2-D_2}} \gamma_{OL}} \quad (17)$$

$$k_B = (k_B)_{\mathbf{2-D}} + \frac{(k_B)_{\mathbf{2-D_2}}\, a_D}{(K_a)_{\mathbf{2-D_2}}} \quad (18)$$

The increase with decreasing pD in the apparent second-order rate constant k_B for deprotonation of **2-D** by DPO_4^{2-} is also due to the appearance of a second reaction pathway for deprotonation of the strong carbon acid **2-D$_2$** by DPO_4^{2-} (Scheme 3). Equation 18 gives the relationship between the apparent rate constants k_B and the rate constants for deprotonation of **2-D** ($(k_B)_{\mathbf{2-D}}$) and **2-D$_2$** ($(k_B)_{\mathbf{2-D_2}}$) by DPO_4^{2-}. The plot (not shown) of k_B (M^{-1} s^{-1}) against a_D is linear. The intercept of this plot gives the second-order rate constant for deprotonation of the iminium ion **2-D** by DPO_4^{2-}, $(k_B)_{\mathbf{2-D}} = 2.8 \times 10^{-2}$ M^{-1} s^{-1} (Table 5). Combining the slope of this plot with $(K_a)_{\mathbf{2-D_2}} = 1.7 \times 10^{-3}$ M (Table 1) gives the second-order rate constant for deprotonation of **2-D$_2$** by DPO_4^{2-}, $(k_B)_{\mathbf{2-D_2}} = 1 \times 10^2$ M^{-1} s^{-1} (Table 5). There is a very large uncertainty in the values of the rate constants estimated for deprotonation of **2-D$_2$** by DO^- and by DPO_4^{2-}. First, there is the inherent uncertainty in the value for $(K_a)_{\mathbf{2-D_2}}$ determined by fitting experimental data from Figure 1 to Scheme 3. Second, there are two carboxylates at **2-D** of uncertain relative basicity which may undergo protonation, and our limited experimental data is not sufficient to distinguish between the two different forms of **2-D$_2$**.

Brønsted Correlations. The Brønsted correlation of second-order rate constants k_B (M^{-1} s^{-1}) for deprotonation of **1-D** (●) shown in Figure 6 was obtained using data from Table 5. The slope of this correlation, $\beta = 0.83 \pm 0.01$, is smaller than the value of $\beta = 0.92 \pm 0.04$ for deprotonation of N-protonated glycine methyl ester (▲) determined in earlier work.[1] The smaller Brønsted β observed for **1-D** compared with N-protonated glycine methyl ester is consistent with a Hammond-type shift to an earlier transition state for deprotonation of the more strongly acidic carbon acid.[31]

Electrophilic Catalysis of Deprotonation of Glycine. A broad goal of this work is to determine the effect of different electrophilic catalysts on the carbon acidity of glycine. Chart 2 shows that formation of an imine between acetone and glycine

(30) Richard, J. P.; Williams, G.; O'Donoghue, A. C.; Amyes, T. L. *J. Am. Chem. Soc.* **2002**, *124*, 2957−2968.

(31) Hammond, G. S. *J. Am. Chem. Soc.* **1955**, *77*, 334−338.

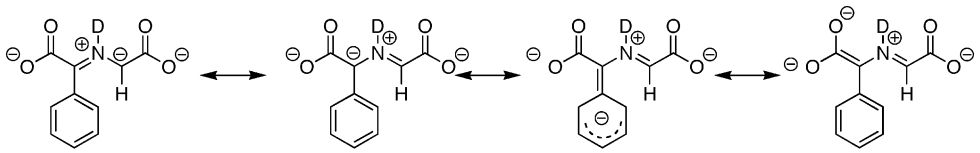

4

Chart 2

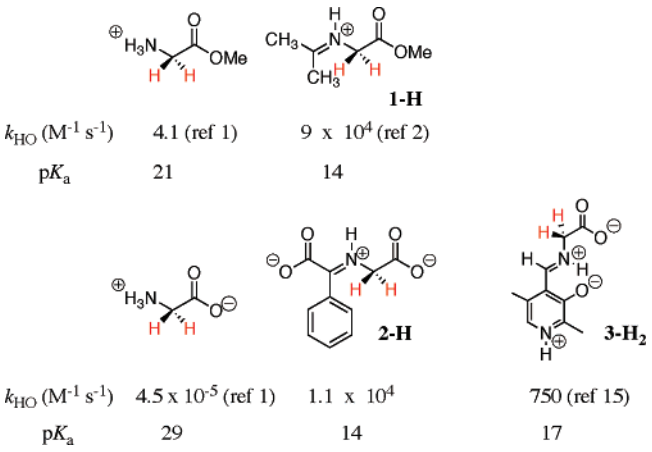

methyl ester causes a healthy 2200-fold increase in the second-order rate constant k_{DO} for deprotonation of the α-amino carbon by deuterioxide ion. This reflects the ca. 7 unit difference in the carbon acid pK_a of 21 for N-protonated glycine methyl ester and of 14 for **1-H**.[2]

The formation of the imine between glycine and phenylglyoxylate causes a much larger 2.2×10^8-fold increase in the second-order rate constant k_{DO} for deprotonation of the α-amino carbon by deuterioxide ion. This is 50-fold larger than the effect of formation of an imine to the oxygen-ionized form of 5′-deoxypyridoxal (Chart 2). Combining $k_{DO} = 1.7 \times 10^4$ M^{-1} s^{-1} for deprotonation of **2-D** with an estimated solvent deuterium isotope effect of $k_{DO}/k_{HO} = 1.5$[32] gives $k_{HO} = 1.1 \times 10^4$ M^{-1} s^{-1} for deprotonation of **2-H** by hydroxide ion in H_2O (Scheme 3). Equation 19 is the linear logarithmic correlation between k_{HO} and the carbon acidity pK_{CH} for deprotonation of cationic ketones and esters.[2]

$$pK_{CH} = \left(\frac{10.2 - \log k_{HO}}{0.44}\right) \qquad (19)$$

This correlation and $k_{HO} = 1.1 \times 10^4$ M^{-1} s^{-1} gives a value of p$K_a = 14$ for the carbon acidity of **2-H**. The carbon acid pK_a for this iminium ion is 15 units smaller than pK_a of 29 for the parent carbon acid glycine,[1] and smaller even than the pK_a of 17 estimated for **3-H$_2$**.[15] By comparison, formation of an imine to acetone causes only a 7 unit reduction in the pK_a of glycine methyl ester.[2] The strong carbon acidity for **2-H** shows the extensive stabilization of negative charge of the carbanion **4** that is presumably due to delocalization of negative charge onto the electron-deficient substituents at **4**.

It is important to distinguish the relative absolute reactivity of the parent carbonyl compounds as catalysts of deprotonation of glycine methyl ester and of glycine, from the relative carbon acidity of the iminium ion adducts to these compounds (Chart 2). In particular, 5′-deoxypyridoxal (DPL) is a much better catalyst of deprotonation of glycine than is phenylglyoxylate anion, despite the weaker carbon acidity of the adduct to glycine (Chart 2). Chart 3 shows a comparison of the rate constants for solvent-catalyzed deprotonation of glycine methyl ester and glycine, and the rate constants observed upon addition of a 0.01 M ketone catalyst. The first row shows that, despite the strong carbon acidity of the iminium ion adduct, 0.010 M acetone provides only modest catalysis of deprotonation of glycine methyl ester at pD 7.6, because of the unfavorable equilibrium constant for imine formation. A 250-fold rate acceleration is observed for catalysis of deprotonation of glycine by 0.010 M of the much more effective catalyst phenylglyoxylate. However, this rate acceleration pales in comparison to the 3,000,000-fold acceleration observed for catalysis of deprotonation of glycine by 0.010 M DPL at pH 7.1, where the estimated rate constant for solvent-catalyzed deprotonation of glycine is only 5×10^{-12} s^{-1}.[1]

The large difference in the observed catalytic activity of DPL and phenylglyoxylate is due to the more favorable equilibrium constant for formation of the imine to the former electrophile (Figure 2). The imine **2-D** is only barely detectable by ^{1}H NMR in solutions that contain molar concentrations of glycine and 0.80 M phenylglyoxylate anion, while the reaction of 0.10 M glycine with 0.010 M DPL at pH 7.1 results in conversion of 80% of the cofactor to **3-H$_2$** at chemical equilbrium.[15] These data show that one imperative for the strong preference of enzyme catalysts to use pyridoxal 5′-phosphate rather than the pyruvoyl prosthetic group[17,18,20] as a coenzyme for catalysis of the reactions of amino acids is the larger affinity of the pyridine cofactor compared with α-keto acids for addition to the amino group to form an imine. This imperative was noted in an earlier study of imine formation to PLP.[33]

We conclude that imines between pyridoxal and amino acids are strongly stabilized by intramolecular interaction between the pyridine ring, the ring substitutents, and the imino nitrogen,[33] compared to the corresponding intramolecular interactions at imines between amino acids and simple ketones and aldehydes. There is an extensive literature on imine formation in water. However, to the best of our knowledge there has been no systematic study reported to rationalize the high stability of imines to PLP compared to imines to simple aldehydes and ketones. This study is currently in progress in the laboratory at the Universidad de Santiago.

Acknowledgment. We acknowledge the National Institutes of Health (Grant GM 39754 to J.P.R.), and the Ministerio de Educación y Ciencia and the European Regional Development

(32) This is the secondary solvent deuterium isotope effect determined for deprotonation of acetone by hydroxide ion at 25 °C [Pocker, Y. *Chem. Ind.* **1959**, 1383−1384].

(33) Gout, E.; Zador, M.; Beguin, C. G. *Nouv. J. Chim.* **1984**, *8*, 243−250.

Chart 3

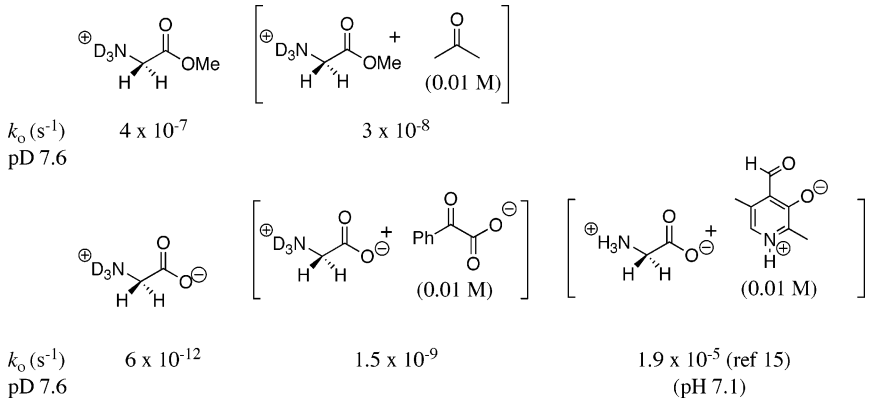

Fund (ERDF) (Grant CTQ2004-06594 to A.R. and J.C.) for generous support of this work.

Note Added after ASAP Publication. Reference 27 was changed after ASAP publication of this article on January 17, 2008. The current version shows the correct reference.

Supporting Information Available: Table S1 of second-order rate constants $(k_B)_{hyd}$ for general base-catalyzed hydrolysis of N-protonated glycine methyl ester; Table S2 of first-order rate constants, k_{ex}, for exchange for deuterium of the first α-proton of glycine methyl ester in the presence of acetone and buffer catalysts; Table S3 of first-order rate constants, k_{ex}, for exchange for deuterium of the first α-proton of glycine in the presence of phenylglyoxylate and buffer catalysts. This material is available free of charge via the Internet at http://pubs.acs.org.

JA078006C